CORROSION-PRODUCTS INDUCED WEDGE EFFECT AND FATIGUE CRACK GROWTH OF STAINLESS STEELS

K. Komai*, S. Murayama and H. Kanasaki*****

**Department of Mechanical Engineering, Kyoto University, Kyoto, Japan*
***Ishikawajimaharima Heavy Industries, Yokohama, Japan*
***Mitsubishi Heavy Industries, Takasago, Japan*

ABSTRACT

In martensitic type stainless steel (SUS410) crack closure behavior was affected by solidlike and viscoelastic corrosion-products induced wedge effect; the load sharing capacity of the former was exclusively effective resulting in a raised stress intensity to close the crack, thereby reducing growth rates. In austenitic type SUS304 no wedge effect was observed. da/dN of the former was accelerated by stress-assisted dissolution and hydrogen embrittlement. da/dN of the latter was accelerated by water molecule adsorption induced reverse slip suppression, in addision to the preceding two factors.

KEYWORDS

Corrosion-products: wedge effect; corrosion fatigue crack growth; stainless steels.

INTRODUCTION

Environmental influences on fatigue crack growth of stainless steels have been discussed in various environments (Speidel, 1977; Amzallag, 1978; Bamford, 1979). The authors have already reported that corrosion-fatigue (CF) crack growth is influenced by corrosion-products induced wedge effect (Endo, 1969), an icrease of crack width and crack tip blunting (Endo, 1975), and superposition of stress corrosion cracking (SCC) (Endo, 1977). The corrosion-products induced wedge effect results in a raised stress intensity required to close the crack, thereby reduing growth rates in a high-tension steel (Endo, 1981, 1983). In the present study, aqueous environment sensitive behavior of CF crack growth has been discussed on martensitic and austenitic stainless steels.

EXPERIMENTAL PROCEDURE

Materials tested was a quench and tempered martensitic (SUS410) and a

solution-treated austenitic (SUS304) stainless steels. SUS410 was quenched from 970°C in oil and tempered at 730°C in air. The chemical compositions and mechanical properties after heat treatments are shown in Tables 1 and 2 respectively. The shape and dimensions of specimens are a usual WOL type (thickness 5.3), where a crack plane orientation was L-T. The load-strain hysteresis loops were measured by an unloading elastic compliance method (Kikukawa, 1976) and a strain gage adhered to the specimen. Data acquisition system by a minicomputer has been reported elsewhere (Endo, 1981).

Dry air (dew point = -70°C, water content < 2 ppm) as a reference environment, 3 - 0.001 % NaCl solution by weight and deionozed water were used as testing environments. The temperature of the solution was kept at 25°C. Cathodic potential of -1.0 V against a saturated calomel electrode (SUS410) or cathodic current of 3 mA/cm^2 (SUS304) was applied by a potentiostat.

EXPERIMENTAL RESULTS AND CONSIDERATIONS

Load-Strain Hysteresis Loop

The hysteresis loops of SUS410 were calssified into 5 types as is shown in Fig. 1. Here the perfect crack opening K (K_{op2}) and the apparent crack closing one (K_{cl}*) were defined as a value which deviated from the horizontal straight line during loading and unloading period respectively. In Fig. 1, D type in dry air and C4 type at f = 0.1 Hz in 1 % NaCl solution are the hysteresis loops having the same paths during loading and unloading period. At f = 10 Hz in 1 % NaCl solution there appeared C1, C2, and C3 type tracing different paths during loading and unloading period, and K_{cl}* was always greater than or equal to K_{op2}.

The changes of hysteresis loops after immersion in 1 % NaCl solution are summarized in Table 3. Under free corrosion at f = 10 Hz, C3 type at R = 0.1 and C2 type at R = 0.5 changed into C2 → C1 and C1 type respectively when the load increased stepwise. Under cathodic protection at f = 10 Hz, the

Table 1 Chemical compositions (mass %)

	C	Si	Mn	P	S	Ni	Cr
SUS410	0.09	0.38	0.33	0.021	0.008		13.06
SUS304	0.06	0.43	1.10	0.031	0.005	8.54	18.28

Table 2 Mechanical properties

	$\sigma_{0.2}$ MPa	σ_B MPa	δ %	ψ %
SUS410	490	649	24	
SUS304	210	640	63	59

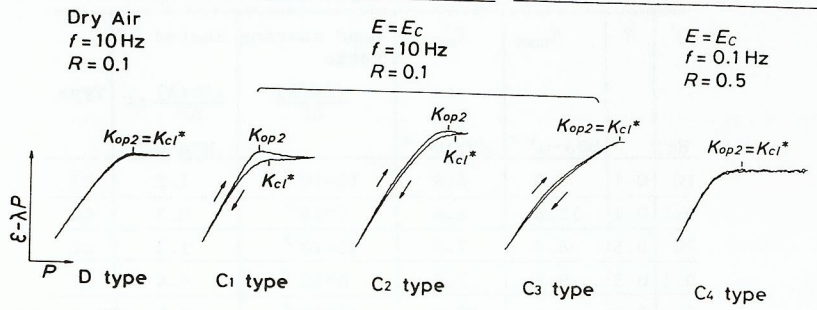

Fig. 1 Classification of hysteresis loops (SUS410).

C1 type remained unchanged in spite of a little rise of K_{op2} and K_{cl}*. At f = 0.1 Hz, however, only D or C4 type tracing the same paths during loading and unloading period appeared. C4 type under free corrosion was followed by D type when the load increased stepwise, but D type under cathodic protection was unchanged. In SUS304 there was observed no influences of cycle frequency, Cl^- concentration and cathodic current on hysteresis loops, and only D type appeared.

Factors Dominating Crack Closure Behavior

The CF crack closure behaviors were considered to be dominated by the plasticity induced crack closure (Elber, 1971) (hereinafter termed as PCC) and the corrosion-products induced wedge effect (Endo, 1969). In SUS304, there was observed only PCC as was no corrosion-products. The wedge effect observed in SUS410 must be classified into two cases: (i) The solidlike corrosion-products induced crack closure (ECC) and (ii) The viscoelastic or viscous corrosion-products induced one (VCC). C1 type hysteresis loop appeared after a short time immersion in corrosive solution and was considered to be affected by VCC. In case of C2 type, it appeared for the first time after corrosion-products adhered to crack walls and ECC in addition to VCC became dominant. When much more corrosion-products was adhered to crack

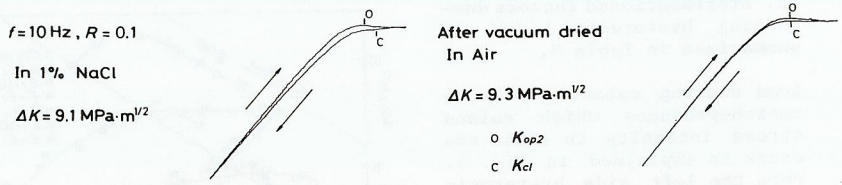

Fig. 2 Hysteresis loops before and after drying in vacuum (SUS410).

Table 3 Changes of hysteresis loops (SUS410)

			Just after immersion	Constant load or Load decrease	Load increase
f = 10 Hz	E=E_C	Type	D→C1	→C2→C3	→C2→C1
	R=0.1	Dominating factors	PCC,VCC,	VCC+ECC, ECC	VCC+ECC,VCC
	E=-1.0V	Type	C1	→C1	→C1
	R=0.1	Dominating factors	VCC,	VCC,	VCC,
	E=E_C	Type	D	→C1→C2	→C1
	R=0.5	Dominating factors	PCC,	VCC, VCC+ECC	VCC,
f = 0.1 Hz	E=E_C	Type	D	→C4	→C4→D
	R=0.1	Dominating factors	PCC,	ECC,	ECC, PCC,
	E=-1.0V	Type	D	→D	→D
	R=0.1	Dominating factors	PCC,	PCC,	PCC,
	E=E_C	Type	D	→C4	→C4→D
	R= 0.5	Dominating factors	PCC,	ECC,	ECC, VCC,

walls, the cracks remained unopened even at a maximum stress resulting in C3 type where ECC became dominant exclusively.

The reason for the hysteresis loop tracing different paths during loading and unloading period lied in VCC. This was certified by the fact that the different paths diminished in air when the specimen showing the different paths in 1 % NaCl solution was dried completely in vacuum. The loops before and after drying in vacuum are shown in Fig. 2. The paths during loading period were unchanged before and after drying and K_{op2} in both loops also unchanged. Thus, during loading period ECC and PCC became dominant with no influences of VCC. There was observed no different paths during loading and unloading period in C4 type, which was due to VCC being negligible small at a low frequency of 0.1 Hz. Aforementioned factors dominating hysteresis loops are summarized in Table 3.

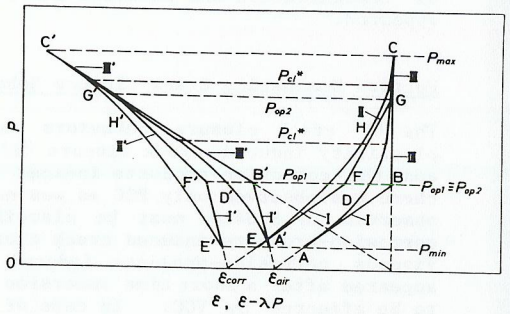

Fig. 3 Load-strain hysteresis loops (SUS410).

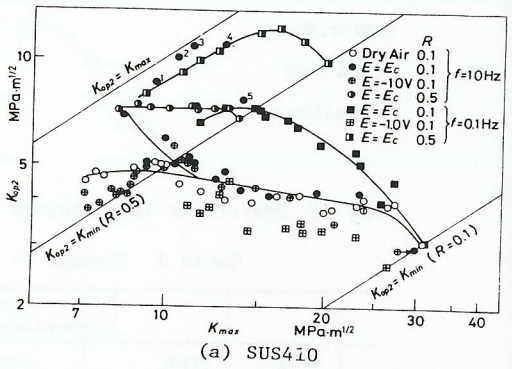

(a) SUS410

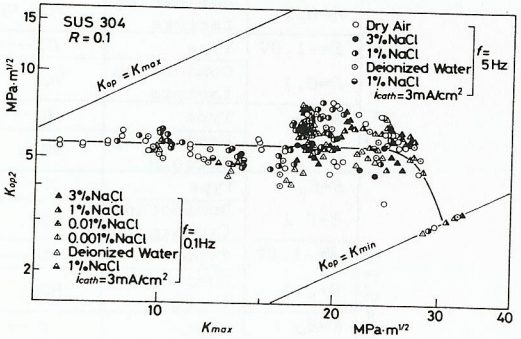

(b) SUS304

Fig. 4 Relations between K_{max} and K_{op2}.

Load sharing capacity of corrosion-products which raised stress intensity to close the crack is explained in Fig. 3. Here the left side hysteresis loops were the original relations between strain (ε) and load (P) and the right ones were those between ($\varepsilon - \lambda P$) and P where elastic deformation (λP) was subtracted from ε so as to parallel an unloading elastic line during crack opening portion to loading axis with the aid of the unloading elastic compliance method. In the figure, the hysteresis loops were divided into three regions of I, II and III fixed the boundaries by the perfect crack closing load P_{op1} and the perfect crack opening one P_{op2}. In Fig. 3, D type affected only by PCC consisted of I and III regions and was approximated by a curve A-B-C-B-A. In C3 or C4 type, the interference of corrosion-products adhered to crack walls brought the region II and the loop was expressed by a curve E-F-G-C-G-F-E. In the original loop the load shared by corrosion-products within cracks could be reduced from the strain difference at perfect crack closing load between C3 or C4 type affected by PCC + ECC (point F') and D affected only by PCC (point B').

In C1 or C2 type dominated by VCC the trace during unloading period differed from the one during loading period owing to viscoelasticity or viscosity of corrosion-products within cracks. Load sharing capacity of VCC was considered in C1 type as follows. When load was supposed to be held at point D' after loading path along A'-B'-C'-D', the point D' was to shift to B' since viscosity effect of corrosion-products was expected to dominish. Under the circumstances there was no difference of strain at a perfect crack closing point between this assumptive loop and the D type one and the load sharing capacity was considered to be identical. Accordingly only the hysteresis loop during loading period was to be considered to evaluate the load sharing capacity of corrosion-products. Moreover, the corrosive solution remained within cracks might share the external load like ECC of the solidlike corrosion-products. The difference of strain before and after drying in vacuum in Fig. 2 was known to be two order small that of ECC. The load sharing capacity of the solution ramained within cracks was negligibly small.

Shared Load by Corrosion-Products and K_{max}-K_{op2} Diagram

The load shared by corrosion-products as ECC was given as $(\Delta\varepsilon/\lambda)$ where $\Delta\varepsilon = \varepsilon_{air} - \varepsilon_{corr}$ in Fig. 3 and the shared K values $(\Delta\varepsilon/\lambda)(\Delta K/\Delta P)$ are shown in Table 4 (SUS410).

Figure 4 (a) illustrates the relation between K_{max} and K_{op2} in SUS410. K_{op2} at f = 0.1 Hz was always higher than that at f = 10 Hz in both cases of R = 0.1 and 0.5 under free corrosion. This might be due to a greater amount of corrosion-products generated within cracks at a smaller da/dt at f = 0.1 Hz. The shared load at f = 10 Hz was, however, much greater than the one at f = 0.1 Hz at almost equivalent K_{op2} (Table 4). Corrosion-products were adhered to almost whole fracture surface including a crack front at f = 10 Hz, whilst at f = 0.1 Hz those were not observed in the vicinity of crack front. The amount of corrosion-products near crack front might have brought the difference of shared load. K_{op2} at f = 0.1 Hz took a higher value at R = 0.5 than at R = 0.1, whilst the shared load at R = 0.1 was equal to the one at R = 0.5. Here crack closing stress became higher

Table 4 Shared load by corrosion-products (SUS410)

f Hz	R	K_{max} MPa·m$^{1/2}$	K_{op2} MPa·m$^{1/2}$	Load sharing ratio $\frac{(\Delta\varepsilon/\lambda)}{\Delta P}$	Shared ΔK $\frac{(\Delta\varepsilon/\lambda)}{\Delta P}\Delta K$ MPa·m$^{1/2}$	Type
10	0.1	8.3	6.9	16×10^{-2}	1.2	C3
0.1	0.1	11.6	6.6	7×10^{-2}	0.7	C4
10	0.5	8.6	7.5	31×10^{-2}	1.3	C2
0.1	0.5	9.2	7.9	8×10^{-2}	0.4	C4
0.1	0.5	12.4	10.6	11×10^{-2}	0.7	C4

owing to a plenty of corrosion-products at R = 0.5, but the shared load at R = 0.5 equaled that at R = 0.1 since the compressive component in the former after crack closure was smaller than that in the latter. Thus K_{op2} was known not necessarily to be corresponded with the shared load. K_{op2} under a cathodic potential at f = 10 Hz and 0.1 Hz nearly coincided with that in dry air, which was due to a scarceness of corrosion-products.

The relation between K_{max} and K_{op2} of SUS304 is shown in Fig. 4 (b). In SUS304 K_{op2} always equaled K_{cl}*. There were observed no influences of cycle frequency, Cl^- concentration and cathodic current on K_{op2}, and a single curve could be drawn between K_{op2} and K_{max}. This corresponded to the fact that there were observed no corrosion-products which rose the K_{op2} on a fracture surface and no crack branching.

da/dN-ΔK, da/dN-ΔK_{eff} Diagram

Figure 5 illustrates the relation between da/dN and ΔK. In SUS410 shown by Fig. 5 (a), da/dN in 1 % NaCl solution at R = 0.1 and f = 10 Hz was accelerated from that in dry air at $\Delta K \geqq 10$ MPa·m$^{1/2}$, but the former became smaller than the latter at $\Delta K < 10$ MPa·m$^{1/2}$ with a higher threshold value than in air due to the corrosion-products induced wedge effect. da/dN at R = 0.5 was greater than that at R = 0.1. da/dN at f = 10 Hz under cathodic potential was equal to that under free corrosion at $\Delta K > 10$ MPa·m$^{1/2}$, but the former became greater than the latter at $\Delta K \leqq 10$ MPa·m$^{1/2}$ with a identical threshold value to ΔK_{th} in dry air.

Fig. 5 (b) illustrates the relation between da/dN and ΔK in SUS304. da/dN in 1 % NaCl solution at f = 5 Hz was accelerated from that in dry air and became 2.5 - 3 times that at $\Delta K \geqq 10$ MPa·m$^{1/2}$. At f = 5 Hz, da/dN in deionized water and NaCl solution of different Cl^- concentration was equal to that in 1 % NaCl solution. A cathodic current (i_{cath}) of 3 mA/cm^2 in 1 % NaCl solution

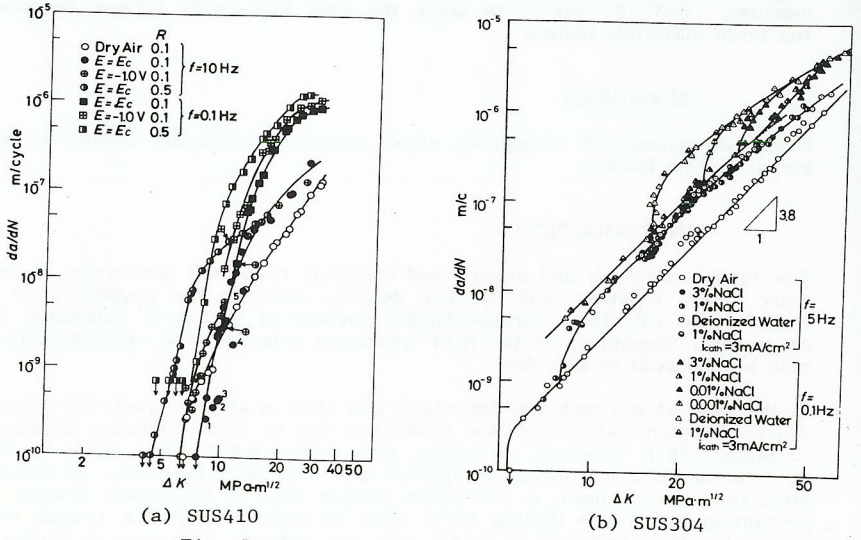

(a) SUS410 (b) SUS304

Fig. 5 Relations between da/dN and ΔK.

either did not change da/dN from that under free corrosion. At f = 0.1 Hz, da/dN in 1 % NaCl solution was 1.3 times that at f = 5 Hz. da/dN in deionized water was equal to that in 1 % NaCl solution at $\Delta K < 15.5$ MPa·m$^{1/2}$ but the former became 2.5 times the latter at $\Delta K \geqq 15.5$ MPa·m$^{1/2}$. da/dN under i_{cath} = 3 mA/cm^2 was the same as that in deionized water.

It might come into question to arrange da/dN in terms of ΔK_{eff} (= $K_{max} - K_{op2}$) since K_{op} did not always give the net load shared by the wedge effect as was mentioned before in addition to a fairly large scattering of the measured values near threshold region. However, useful conclusions could be still drawn out from da/dN-ΔK_{eff} diagram. Fig. 6 illustrates the relation between da/dN and ΔK_{eff} in SUS410. The influence of stress ratios observed under free corrosion in Fig. 5 (a) was eliminated, and a single curve was obtained at both frequencies. da/dN in 1 % NaCl solution at f = 10 Hz always accelerated from that in dry air followed by a further increase at $\Delta K > 6$ MPa·m$^{1/2}$.

Accelerating Mechanism

SUS410 Trace of corrosion was always observed more or less on fracture surfaces at any conditions including cathodic protection. Therefore, stress-assisted dissolution was known to accelerate da/dN from that in dry air. The fracture surface at f = 0.1 Hz under free corrosion was the most severely corroded and so many corrosion pits were observed. Under free corrosion the further acceleration of da/dN at f = 10 Hz and $\Delta K_{eff} > 6$ MPa·m$^{1/2}$ was well corresponded to the increase of intergranular and brittle transgranular fracture area fractions indicating the acceleration to be due to hydrogen embrittlement (HE). At f = 0.1 Hz, however, the acceleration of da/dN did not correspond with the fracture area fraction, which might be due to the abrupt increase of stress-assisted dissolution. Cathodic protection had no effect at f = 10 Hz and $\Delta K_{eff} > 5$ MPa·m$^{1/2}$ and at f = 0.1 Hz and $\Delta K_{eff} > 14$ MPa·m$^{1/2}$. Cathodic protection was effective at f = 10 Hz and $\Delta K_{eff} < 5$ MPa·m$^{1/2}$ resulting da/dN to be equal to that in dry air.

SUS304 No influences of Cl^- concentration and of cathodic current in an acceleration process of da/dN in aqueous environment were observed. Almost whole surface was occupied by ductile transgranular cracking as in dry air with no trace of corrosion. Consequently the acceleration of da/dN in aqueous environment was attributable not to the stress-assisted dossolution at crack tips but to an adsorption effect of water molecule on a newly exposed fresh surface at crack tips. An increased ΔK-value resulted in an increased crack opening period, that was, an exposure period of newly formed slip steps at crack tips to an environment. Therefore, the adsorption layer of water molecule was tightly formed, with a reduced reverse slip during an unloading period in a cycle. A more tightly adsorbed layer at f = 0.1 Hz than that at f = 10 Hz resulted in a more reduced reverse slip, thereby accelerating the da/dN. A crack opening period was dependent only on K_{max}

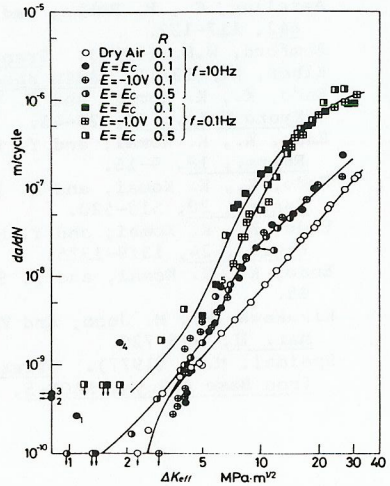

Fig. 6 Relations between da/dN and ΔK_{eff}

and independent of the environment. Therefore, K-value which started to accelerate da/dN in aqueous environment did not depend upon Cl^- concentration but upon cyclic frequency, and da/dN was accelerated at a lower ΔK with a lowering of freqeuncy.

da/dN in deionized water at f = 0.1 Hz was accelerated again under ΔK = 15.5 MPa•m$^{1/2}$, which resulted from HE of plasticity-induced martensite formed around crack tips. da/dN in 3 % NaCl solution at f = 0.1 Hz was accelerated again under ΔK = 30 MPa•m$^{1/2}$ by stress-assisted dissolution of active slip steps at crack tips. Corrosion trenches and pits caused by a tunnelling corrosion were observed on the whole fracture surface.

CONCLUSIONS

(1) In a martensitic stainless steel SUS410, crack closure behavior is affected by plasticity induced crack closure (PCC), corrosion-products induced crack closure as solid properties (ECC) and as viscoelastic properties (VCC). On the other hand, in an austenitic stainless steel SUS304, only PCC is observed as is no corrosion products, and the crack closure behavior is independent upon environmental conditions and cycle frequencies.
(2) The load sharing capacity of the wedge effect as VCC is negligibly small, whilst that as ECC is exclusively effective resulting in a raised stress intensity to close the crack, thereby reducing growth rates.
(3) da/dN of SUS410 is accelerated by stress-assisted dissolution and hydrogen embrittlement (HE).
(4) In SUS304, the near threshold acceleration of da/dN in aqueous environment from that in dry air is considered to be due to the water molecule adsorption induced reverse slip suppression. The second acceleration at a low frequency is due to HE of a plasticity-induced martensite formed at crack tips.

REFERENCES

Amzallag, C., P. Rabbe, and A. Desestret, (1978). ASTM Spec. Tech. Publ., 642, 117-132.

Bamford, W.H., (1979). Trans. ASME, J. Press Vessel Tech., 101, 73-79.

Elber, W., (1971). ASTM Spec. Tech. Publ., 486, 230-242.

Endo, K., K. Komai, and K. Ohnishi, (1969). Memoirs of Faculty of Engng., Kyoto Univ., 31, 25-46.

Endo, K., K. Komai, and Y. Suzuki, (1975). Bulletin of Japan Soc. Mech. Engrs., 18, 9-16.

Endo, K., K. Komai, and N. Imashiro, (1977). Bulletin of Japan Soc. Mech. Engrs., 20, 513-520.

Endo, K., K. Komai, and Y. Matsuda, (1981). Bulletin of Japan Soc. Mech. Engrs., 24, 1319-1325.

Endo, K., K. Komai, and T. Shikida, (1983). ASTM Spec. Tech. Publ., 801, 81-95.

Kikukawa, M., M. Jono, and K. Tanaka, (1976). Proc. Intern. Conf. Mech. Behav. Mat. II, 716-720.

Speidel, M.O. (1977). Stress Corrosion Craking and Hydrogen Embrittlement of Iron Base Alloys, NACE-5, 1071-1094.